Journal of Applied Mathematics and Physics, 2025, 13(6), 2170-2181
https://www.scirp.org/journal/jamp
ISSN Online: 2327-4379
ISSN Print: 2327-4352

# Analysis of Vehicle End Noise under Higher Speed Operating Conditions of a High-Speed Train Based on OTPA

**Guangliang Pan, Yanju Zhao, Dawei Chen**

CRRC Qingdao Sifang Co., Ltd., Qingdao, China
Email: Pangl_qd@126.com

**How to cite this paper:** Pan, G.L., Zhao, Y.J. and Chen, D.W. (2025) Analysis of Vehicle End Noise under Higher Speed Operating Conditions of a High-Speed Train Based on OTPA. *Journal of Applied Mathematics and Physics*, **13**, 2170-2181.
https://doi.org/10.4236/jamp.2025.136123

**Received:** May 14, 2025
**Accepted:** June 27, 2025
**Published:** June 30, 2025

## Abstract

Based on field test, the noise characteristics inside A high-speed train under higher speed conditions above 350 km/h were tested and analyzed. The distribution of noise sources inside the train, the contribution of interior panels, and the contributions of airborne and structural-borne sound to in-vehicle end noise were studied. The test results show that under higher speed conditions, the significant frequency band of interior noise is in the 1/3 octave band of the center frequency of 100 - 300 Hz and the main source of noise comes from the passenger compartment floor. The main source of noise inside the vehicle is the transmission of wheel rail vibration through the center pin, anti-yaw absorber, and air suspension to the vehicle body, which is then radiated by the vibration of the interior panels. Therefore, suppressing low-frequency structural vibration and sound transmission of the floor is an effective method to reduce noise inside the vehicle.

## Keywords

Vehicle End Noise, OTPA Analysis, High-Speed Train

## 1. Introduction

In recent years, while high-speed trains have developed rapidly in China, there issues with noise and vibration have become increasingly prominent [1] [2]. With the proposal of a standard operating speed goal of 400 kilometers per hour (km/h), the noise level inside the train has become a crucial design parameter for vehicle design. To meet the design requirements for interior noise levels, identifying the sources of noise in high-speed trains and determining their contributions has become a necessary means for acoustical optimization in high-speed rail [3].

For complex mechanical structures, there are often multiple different sources of noise and vibration, and each source transmits to the response point through different paths. Transfer Path Analysis (TPA) suggests that the contributions from different paths form the total response. Therefore, the transfer path is associated with the partial contributions from each exciting source. Determining the proportion of contributions transmitted through different paths to the response point can identify the main sources of noise inside the train car, providing a feasible reference for controlling interior noise. However, traditional Transfer Path Analysis has the following issues: measurements for individual transfer paths are affected by changes in boundary conditions, and the measurement process is complex, resulting in a large overall measurement quantity. Operational Transfer Path Analysis (OTPA) under operating conditions is an improvement on traditional path analysis, using real-time excitation as a reference signal to characterize the original load excitation signal. Compared to traditional TPA, OTPA is characterized by its simplicity and time-saving features [4].

## 2. OTPA Theory and Experimental Methods

### 2.1. The Theory of OTPA

The passenger compartment of high-speed trains is a relatively enclosed environment, where internal vibration and noise often involve multiple excitation sources that propagate through various paths, attenuate within the car, and form a complex acoustic environment after multiple reflections. OTPA is developed based on traditional TPA, and its expression is:

$$Y(j\omega) = H(j\omega) \times (j\omega) \tag{1}$$

In this equation, Y(jω) represents the output vector at the response point; X(jω) represents the input vector at the excitation point; H(jω) represents the operational transfer function matrix. In the analysis of noise and vibration transfer paths, the input from the excitation source often includes vibration, force, or sound pressure signals. Therefore, the input and output variables in the above equation can be expressed in the following form:

$$\mathbf{Y} = \begin{bmatrix} a_y \\ f_y \\ p_y \end{bmatrix}, \quad \mathbf{X} = \begin{bmatrix} a_x \\ f_x \\ p_x \end{bmatrix} \tag{2}$$

where, $a_y = \left(a_y^{(1)} \quad \cdots \quad a_y^{(k)}\right)$, $a_x = \left(a_x^{(1)} \quad \cdots \quad a_x^{(l)}\right)$ are the output/input acceleration vector; $f_y = \left(f_y^{(1)} \quad \cdots \quad f_y^{(m)}\right)$, $f_x = \left(f_x^{(1)} \quad \cdots \quad f_x^{(n)}\right)$ are the output/input force vectors; $p_y = \left(p_y^{(1)} \quad \cdots \quad p_y^{(o)}\right)$, $p_x = \left(p_x^{(1)} \quad \cdots \quad p_x^{(p)}\right)$ are the output/input sound pressure vectors; k, l, m, n, o and p represent the number of measurement points for each type of physical quantity.

Therefore, in OTPA, multiple physical variables of all excitation sources during one experiment operation can be taken as inputs vector, and the transfer relationship between the source and response point can be established:

$$\begin{bmatrix} y^{(1)} & \cdots & y^{(n)} \end{bmatrix} = \begin{bmatrix} x^{(1)} & \cdots & x^{(m)} \end{bmatrix} \begin{bmatrix} H_{11} & \cdots & H_{1n} \\ \vdots & \ddots & \vdots \\ H_{m1} & \cdots & H_{mn} \end{bmatrix} \tag{3}$$

where $m$ and $n$ are respectively the number of input and response measurement variables.

By measuring the physical quantities of the excitation and response points during experiment, it is convenient to construct the input and response sample matrices. Therefore, the transfer function matrix of the system under operation conditions can be easily solved based on Equation (1).

$$\mathrm{H} = \mathrm{X}^{-1}\mathrm{Y} \tag{4}$$

The H matrix is the matrix that links the measured physical quantities of various input sources under operating conditions to the output response points. Through this matrix, it is possible to quantitatively analyze the contributions of each source/transfer path to the output response points.

## 2.2. Analysis of Interior Noise

The high-speed train which was tested consists of 8 cars, using a distributed power unit with 4 powered cars and 4 trailer cars, with auxiliary equipment located at the bottom of the vehicles. To study the problem of cabin interior noise, it is necessary to first determine the noise level in the target analysis area. This study focuses on the interior noise at the end of the middle car of the train, with measurement points located on the centerline of the longitudinal axis of the passenger compartment, at a height of 1.2 m from the passenger compartment floor. The measured quantity is the A-weighted equivalent continuous sound pressure level, with a measurement time of more than 20 seconds. This experiment was conducted on a concrete ballastless track slab, and on a straight track. A-weighted equivalent continuous sound pressure level, in decibels, given by:

$$L_{pAeq,T} = 10 \cdot \log\left(\frac{1}{T}\int_0^T \frac{p_A^2(t)}{p_0^2}\right) \tag{5}$$

where $p_A$ is the A-weighted sound pressure and $T$ is the measurement time interval. dB reference level is $2 \times 10^{-5}$ Pa [5].

When the vehicle's operating speed increased from 350 km/h to 400 km/h, the interior noise level increased by approximately 3 dB, as shown in **Figure 1**. It can be observed in the figure that within the 1/3 octave band of a center frequency of 50 - 10 kHz, the interior noise increased by 2 - 3 dB, with the main peak frequency range concentrated in the 100 - 315 Hz band. The noise within the 20 - 400 Hz band was analyzed using Fast Fourier Transform (FFT) and its frequency spectrum is shown in **Figure 2**. As seen in the figure, there was a single-frequency peak noise at 154 Hz when operating at 350 km/h. When the speed increases to 400 km/h, the interior noise of 100 - 200 Hz become prominent, with single-frequency peak noise observed at 176 Hz and 194 Hz, which is related to factors such as the vehicle's diameter, track sleeper spacing, and motor drive ratio.

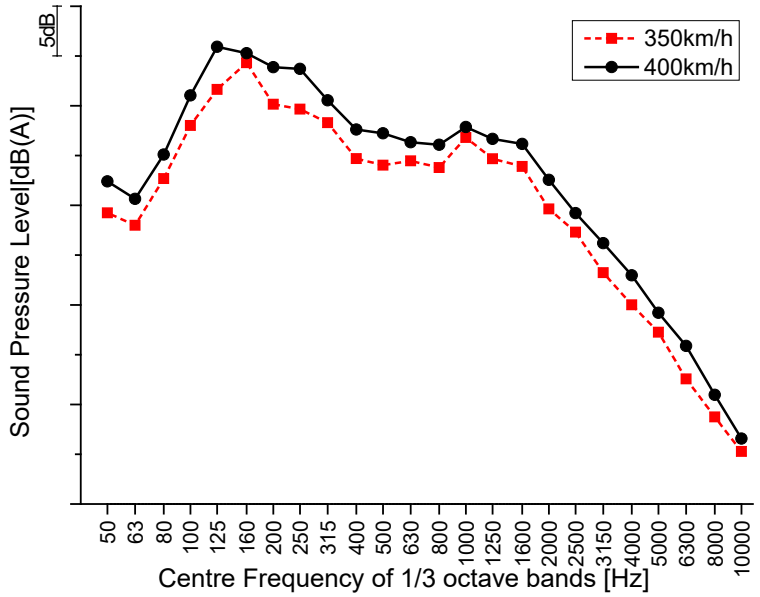


**Figure 1.** The interior end noise level.

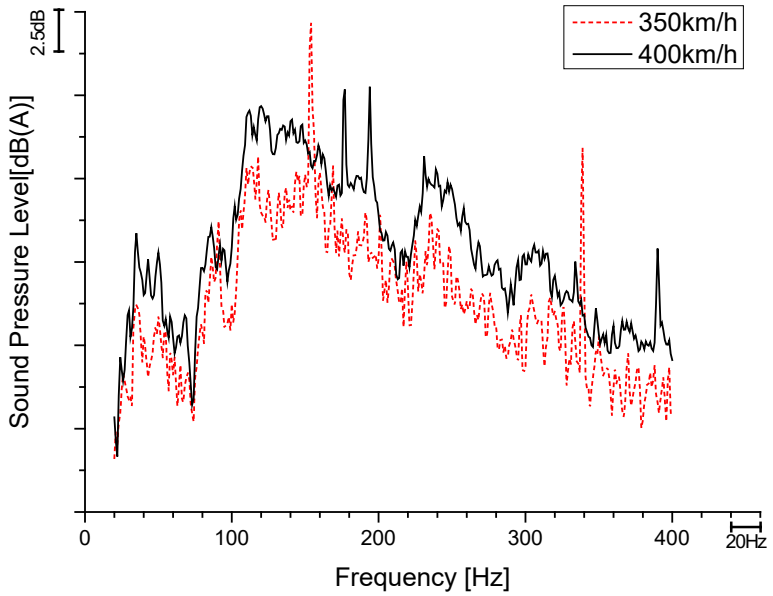


**Figure 2.** FFT spectrum of interior end noise.

## 2.3. Field Testing of Interior Noise

The interior noise can be divided into 2 main forms based on the energy transmission path of the excitation source (including vibration source and noise source): airborne sound transmission and structure-borne sound transmission. Airborne sound transmission refers to the path through which the excitation source is transmitted through the air fluid medium, mainly related to the noise source intensity, the sealing performance of the car body, and the sound insulation characteristics of the trim panels. Structure-borne sound transmission refers to the path through which the excitation source is transmitted through the structural solid medium,

mainly related to the vibration source intensity, the structural characteristics of the car body, and the vehicle suspension parameters [6]. In this paper, the vehicle was tested under unloaded conditions, with an operating speed of 400 km/h. The noise from the bogie under the vehicle is equivalent to the aerodynamic noise of the sidewalls and roof. Therefore, both airborne sound transmission and structure-borne sound transmission have a significant impact on the interior noise of the car. As a result, both types of noise sources need to be tested.

According to the analysis requirements in Section 2.2, the region above the bogie at the end of the high-speed train is determined as the OTPA target analysis area, as shown in **Figure 3**. In order to determine the level of the external noise source and the contribution of the trim to the target point, 12 vibration accelerometers are arranged on the rim of the target analysis area. The locations of the measuring points include the passenger compartment floor, water deflector, side wall under the window, window, luggage rack top plate, and middle top plate, as shown in **Figure 4**. The detailed locations are shown in **Table 1**.

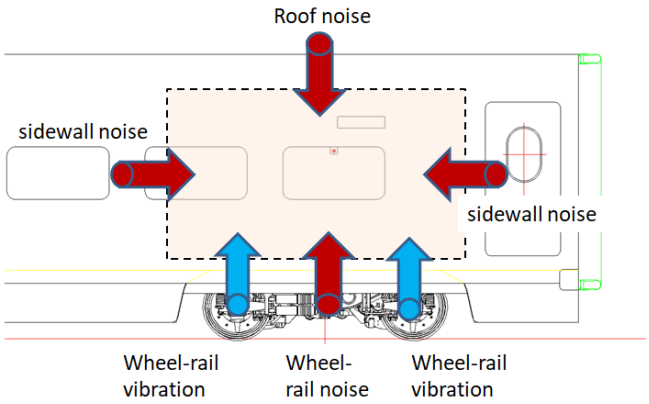


**Figure 3.** Target analysis area of OTPA.

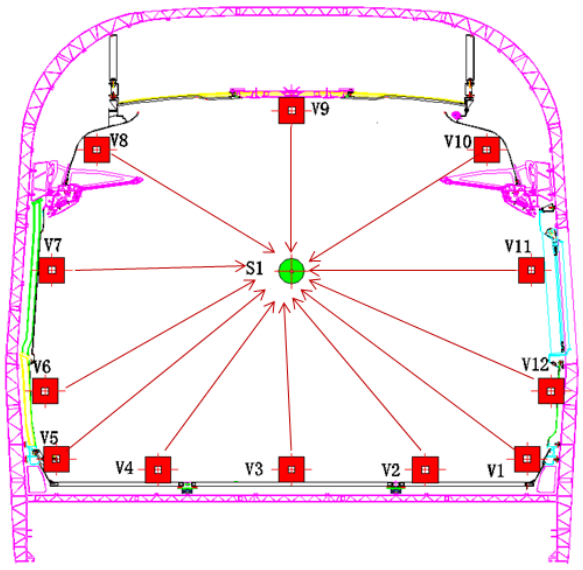


**Figure 4.** Analysis of the contribution of trim.

**Table 1.** Vibration measurement position of trim.

| Points | Measured type | Position of the measurement | Points | Measured type | Position of the measurement |
|---|---|---|---|---|---|
| S1 | Noise | Point at a height of 1.2 m | | | |
| V1 | Vibration | Water deflector panel | V7 | Vibration | Window |
| V2 | Vibration | Passenger compartment floor | V8 | Vibration | Luggage rack top plate |
| V3 | Vibration | Passenger compartment floor | V9 | Vibration | Middle top plate |
| V4 | Vibration | Passenger compartment floor | V10 | Vibration | Luggage rack top plate |
| V5 | Vibration | Water deflector panel | V11 | Vibration | Window |
| V6 | Vibration | Lower sidewall | V12 | Vibration | Lower sidewall |

Regarding the external noise source intensity, we tested the vibration and noise of the bogie area, the side wall noise, and the roof noise. The source intensity of the bogie area includes the vibration and noise of the motor and gearbox equipment, as well as the vibrations in the three Cartesian coordinate directions of the center pin, air spring, anti-yaw vibration absorber, and the axle box, as well as the wheel-rail noise. Please refer to **Figure 5** for details.

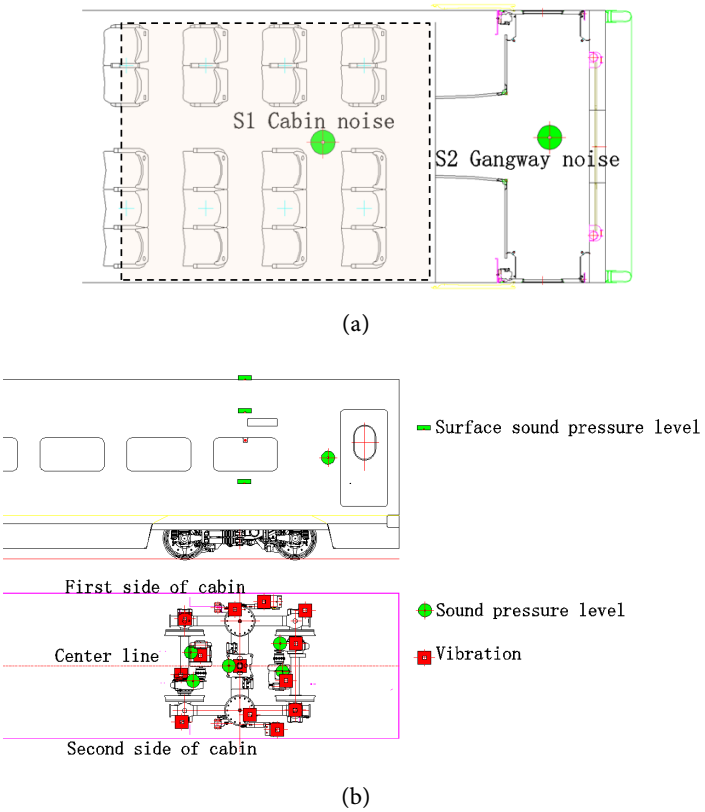


**Figure 5.** Layout of measurement points for noise sources. (a) Interior noise measurement points; (b) External noise measurement points.

## 3. Results and Discussion

### 3.1. Analysis Model of OTPA

In order to obtain an accurate and reliable OTPA model, the experimental test conditions include acceleration, constant speed, coasting, and braking conditions. Each condition undergoes 2 - 3 sets of tests. The data obtained under these different conditions are subjected to Crosstalk Cancellation (CTC) interference correction and Principal Component Analysis (PCA) analysis to determine the contribution of each path. Then, the transfer path matrix is obtained through the TPS (Transfer Path Analysis) process to identify the main noise sources, as shown in **Figure 6**.

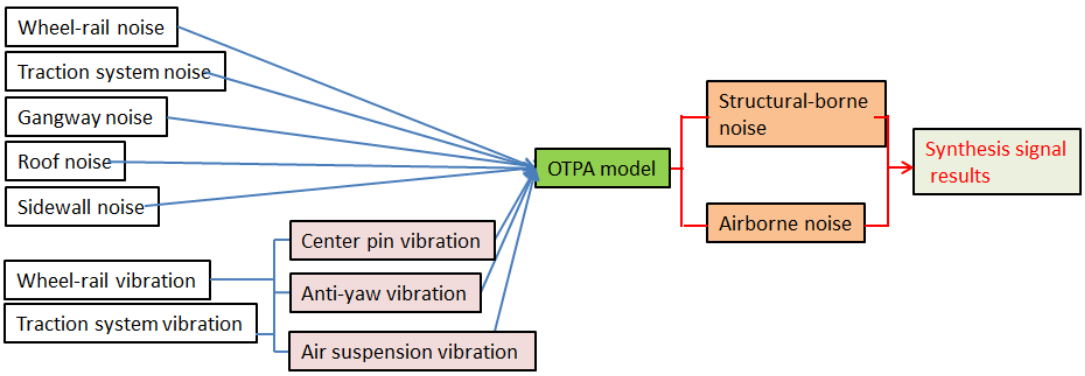


**Figure 6.** Operational transfer path analysis model.

### 3.2. Analysis Results of Panel Contribution

The calculation results of the interior noise level are synthesized by the vibration acceleration data of the passenger compartment ceiling, side roof panel, window partition wall panel, window glass, lower wall panel, drip shield, floor, and compared with the interior test results, as shown in **Figure 7**. The total value of the experiment is 72.8 dB(A), while the synthesized result is 72.3 dB (A), with a calculation error of 0.5 dB. The spectral consistency within the main peak frequency range of 100 - 315 Hz shows a good agreement between calculation and experimental results.

The prominent frequency range of the interior noise is within the 1/3 octave band with a center frequency of 100 - 315 Hz. The total value of the panel contribution indicates that the lower sidewall, floor, and roof panel make significant contributions to this frequency band. Further analysis of the frequency results reveals that the lower sidewall contributes significantly in the 20 - 40 Hz, while the interior floor contributes more prominently in the 100 - 200 Hz band. See **Figure 8** for details.

### 3.3. Analysis Results of External Vehicle Sources

Based on the analysis results in section 3.2, the vibration of the floor contributes significantly to the interior noise within the 100 - 200 Hz frequency band.

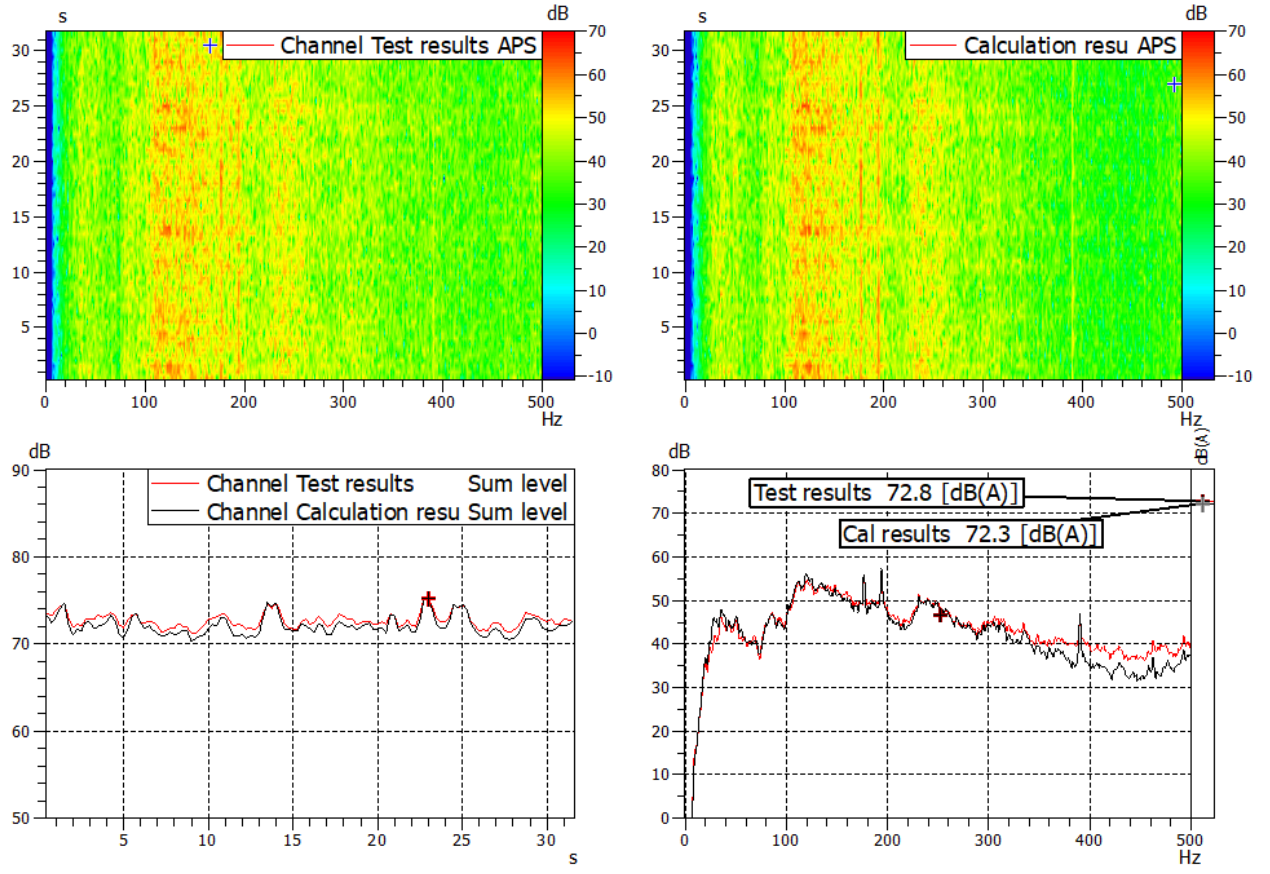


**Figure 7.** Verification of OTPA model for panel contribution

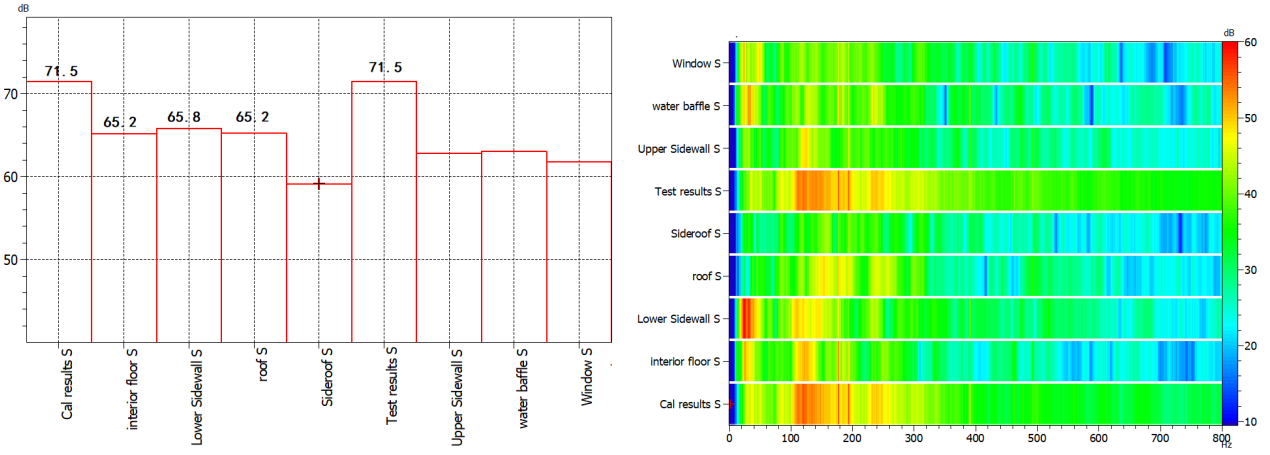


**Figure 8.** Total panel contribution results for the 50 - 315 Hz. Frequency band of interior noise.

Therefore, the vibration of the interior floor V3 is selected as the target response point for OTPA analysis. The main sources of interior floor vibration include:

(1) Vibration and noise from the bogie and traction system are transmitted through the center pin, air suspension, and anti-yaw vibration absorber to the car body, and then transmitted to the interior floor.

(2) Aerodynamic noise from the exterior sidewalls and roof is transmitted

through the car body to the interior floor.

**Table 2.** Measurement points of external sources.

| Points | Measured type | Position of the measurement | Points | Measured type | Position of the measurement |
|---|---|---|---|---|---|
| S2 | Noise | Gangway noise | S13 | Noise | roof noise |
| S3 | Noise | 3-axis gearbox noise | V13 | Vibration | 1st anti-yaw |
| S4 | Noise | 3-axis motor noise | V14 | Vibration | 1st air suspension |
| S5 | Noise | Noise above 3-axis | V15 | Vibration | 2nd anti-yaw |
| S6 | Noise | 4-axis gearbox noise | V16 | Vibration | 2nd air suspension |
| S7 | Noise | 4-axis motor noise | V17 | Vibration | 3-axis axle box |
| S8 | Noise | Noise above 4-axis | V18 | Vibration | 4-axis axle box |
| S9 | Noise | Upper part noise of 1st sidewall | V19 | Vibration | 4-axis gearbox |
| S10 | Noise | Lower part noise of 1st sidewall | V20 | Vibration | 4-axis motor |
| S11 | Noise | Upper part noise of 2nd sidewall | V21 | Vibration | Center pin |
| S12 | Noise | Lower part noise of 2nd sidewall | | | |

Comparing the synthesis results of OTPA with the experimental test results, it can be seen that the main spectral characteristics of the synthesized results match well with the test results. This indicates that the synthesized results can effectively reflect the transfer characteristics of the target vibration point, as shown in **Figure 9**, dB reference level is 1 μm/s$^2$.

In **Figure 10**, the x direction represents the longitudinal direction of the vehicle, the running direction is positive, and vice versa is negative. The y direction represents the lateral direction of the vehicle, pointing to the left is positive, and vice versa is negative. The z direction represents the vertical direction of the vehicle, pointing to the roof is positive, and vice versa is negative. The detailed locations of each region in Figure 10 are shown in **Table 2**.

From the results shown in **Figure 10** and **Figure 11**, it is evident that the vibration of the cabin floor is primarily caused by structural vibration, with airborne noise contributing minimally to floor vibration. The contribution of bogie to the vibration of the end cabin floor through dampers is in the following order: center pin > air suspension > anti-yaw absorber.

## 4. Conclusions

Based on field tests, the study analyzed the characteristics of interior noise at the ends of the passenger compartments of a High-Speed Train operating at a speed of 400 km/h and investigated the contributions of airborne noise and structural-

borne noise to interior noise. The main conclusions are as follows:

(1) At a speed of 400 km/h, the significant frequency band of noise at the end of the passenger compartment inside the vehicle is one-third of the frequency band of 100 - 315 Hz;

(2) According to the analysis of the contribution of trim it can be concluded that the main source of interior noise in the above frequency range is related to floor vibration;

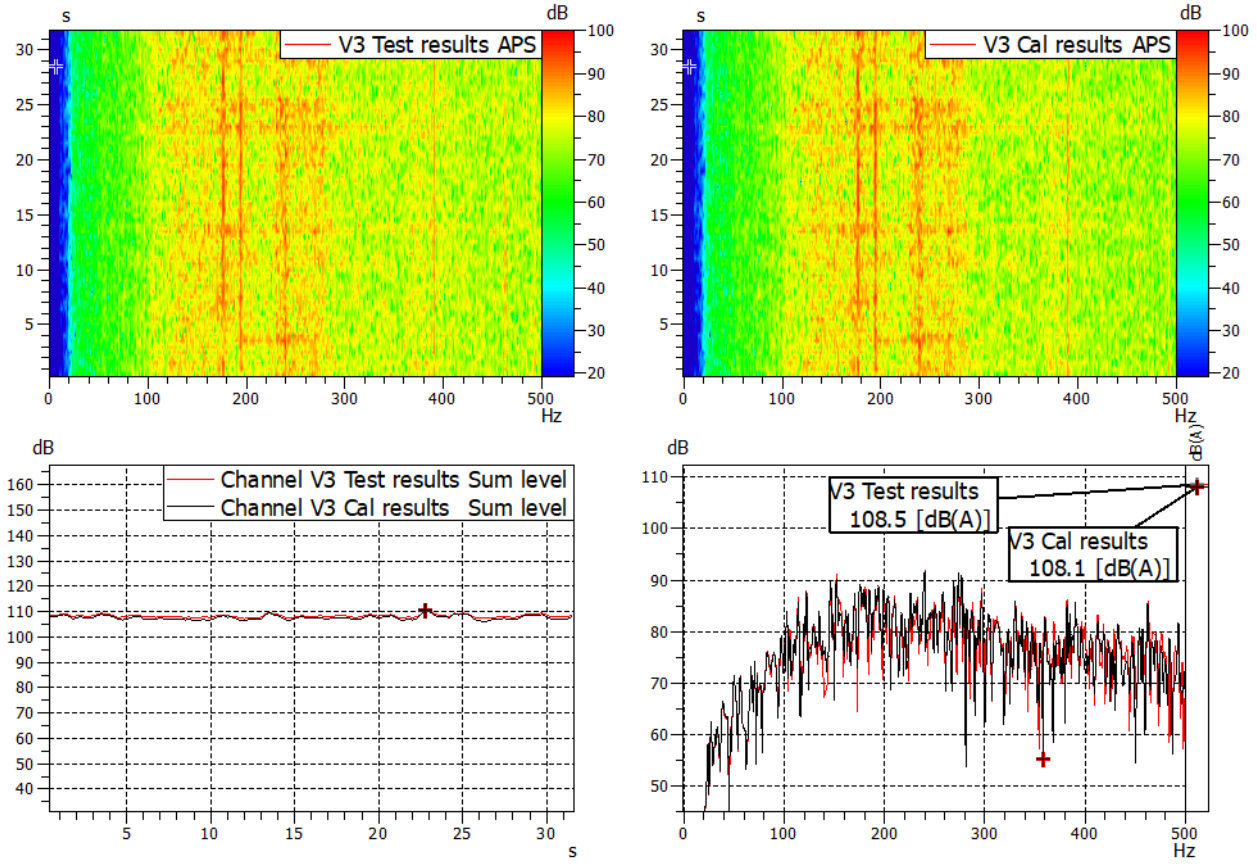


**Figure 9.** Verification of OTPA model for exterior noise.

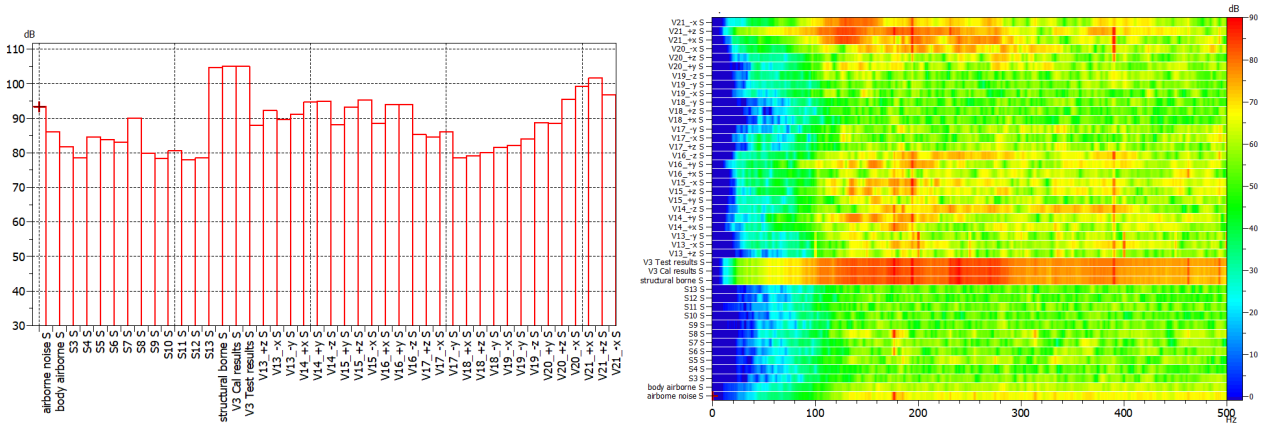

**Figure 10.** The total contribution of each path to the V3 vibration point (50 - 500 Hz).

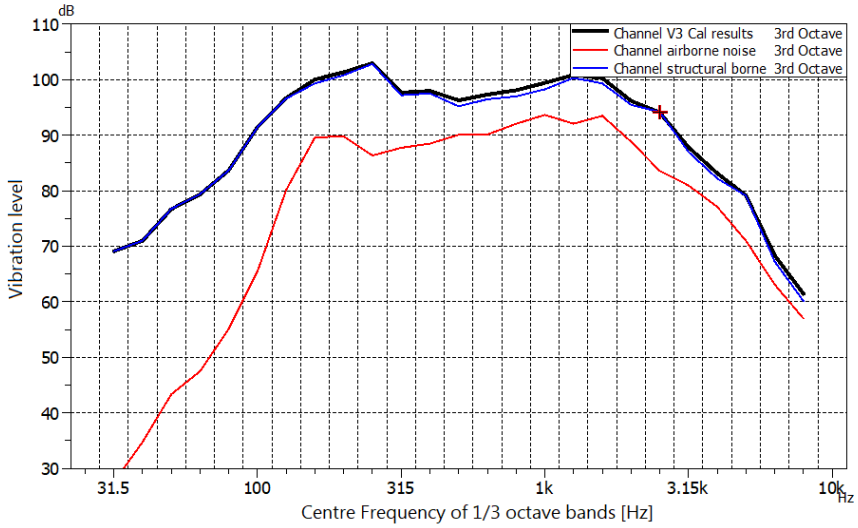


**Figure 11.** The spectral of structural-borne noise and airborne noise to the Vibration of the cabin floor.

(3) The vibration of the wheel-rail and motor tracking system is mainly transmitted to the interior of the vehicle through the center pin and damper, and its contribution order is: Center pin > air suspension > anti-yaw absorber.

Given the above conclusions, inhibiting low-frequency structural vibration and sound transmission of the cabin floor is an effective method for reducing interior noise, especially inhibiting the vibration transmission of center pin, which contributes significantly to interior noise.

## Acknowledgements

The project was supported by the Railway Basic Research Joint Fund of the National Natural Science Foundation of China and China State Railway Group Co., Ltd. (No. U2468226).

## Conflicts of Interest

The authors declare no conflicts of interest regarding the publication of this paper.

## References

[1] Yuan, M.M., Shen, A., Lu, F., *et al.* (2013) Operational Transfer Path Analysis and Noise Sources Contribution for China Railway High-Speed (CRH). *Journal of Vibration and Shock*, **32**, 189-196.

[2] Guo, W.Q. (2014) Analysis of Noise Transmission Path at the End of High-Speed Train Passenger Compartments. *Railway Locomotive and Motor Car*, **480**, 31-33.

[3] Guo, S.H., Liu, Z.G., Zang, X.M., *et al.* (2016) Transfer Path Analysis under Loading Conditions. *Noise and Vibration Control*, **36**, 104-107.

[4] Lu, Y.Y., Cheng, W., Lu, J.T., *et al.* (2015) Research Progress of Operational Transfer Path Analysis Method. *Journal of Hebei University of Science and Technology*, **36**, 359-367.

[5] Yan, L., Chen, Z., Zou, Y.F., *et al.* (2022) Field Study of the Interior Noise and Vibration of a Metro Vehicle Running on a Viaduct: A Case Study in Guangzhou. *International Journal of Environmental Research and Public Health*, **17**, Article 2807. https://doi.org/10.3390/ijerph17082807

[6] Zhang, J., Xiao, X.B., Zhang, Y.M., *et al.* (2015) Study on Transfer Path Characteristic of Interior Noise of 100% Low-Floor Railway Train. *Journal of Vibration Engineering*, **28**, 541-549.